JACS
JOURNAL OF THE AMERICAN CHEMICAL SOCIETY
Article
pubs.acs.org/JACS
Open Access on 07/28/2015

A Fibril-Like Assembly of Oligomers of a Peptide Derived from β-Amyloid

Johnny D. Pham, Ryan K. Spencer, Kevin H. Chen, and James S. Nowick*

Department of Chemistry, University of California, Irvine, Irvine, California 92697-2025, United States

Supporting Information

ABSTRACT: A macrocyclic β-sheet peptide containing two nonapeptide segments based on $A\beta_{15-23}$ (QKLVFFAED) forms fibril-like assemblies of oligomers in the solid state. The X-ray crystallographic structure of macrocyclic β-sheet peptide **3** was determined at 1.75 Å resolution. The macrocycle forms hydrogen-bonded dimers, which further assemble along the fibril axis in a fashion resembling a herringbone pattern. The extended β-sheet comprising the dimers is laminated against a second layer of dimers through hydrophobic interactions to form a fibril-like assembly that runs the length of the crystal lattice. The second layer is offset by one monomer subunit, so that the fibril-like assembly is composed of partially overlapping dimers, rather than discrete tetramers. In aqueous solution, macrocyclic β-sheet **3** and homologues **4** and **5** form discrete tetramers, rather than extended fibril-like assemblies. The fibril-like assemblies of oligomers formed in the solid state by macrocyclic β-sheet **3** represent a new mode of supramolecular assembly not previously observed for the amyloidogenic central region of Aβ. The structures observed at atomic resolution for this peptide model system may offer insights into the structures of oligomers and oligomer assemblies formed by full-length Aβ and may provide a window into the propagation and replication of amyloid oligomers.

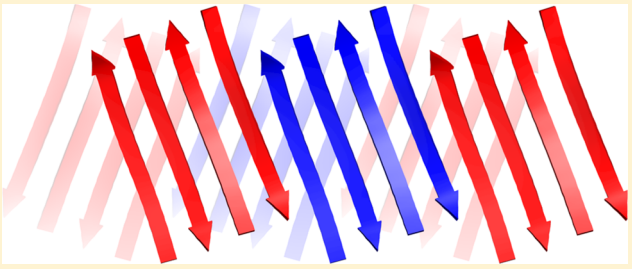

INTRODUCTION

The supramolecular assembly of the β-amyloid peptide Aβ to form fibrils and soluble oligomers has been the subject of intense interest and study over the past two decades. The plaques formed by the 40−42 amino acid Aβ polypeptide in the brain are one of the most distinctive physiological features of Alzheimer's disease, while the more cryptic soluble Aβ oligomers that also form are now thought to be the primary culprits in the devastating neurodegeneration that occurs.[1] In β-amyloid fibrils, the central region of Aβ forms an extended network of β-sheets.[2] The oligomers also appear to involve β-sheet formation, but their structures are still largely unknown at atomic resolution.[3,4] Enhanced understanding of the structures and interactions of the oligomers and fibrils offers the promise of preventing and treating Alzheimer's and other amyloid diseases.

The highly amyloidogenic central region of Aβ, which includes the hydrophobic pentapeptide sequence LVFFA ($A\beta_{17-21}$) has provided an archetype not only for the assembly of Aβ but also for amyloidogenic peptides and proteins in general.[5] This region is particularly prone to interaction, and peptides derived from $A\beta_{17-21}$ have been found to inhibit the aggregation of full length Aβ.[6] The hydrophobic residues 17−21 are flanked by cationic and anionic residues K_{16} and E_{22}, making the heptapeptide sequence KLVFFAE ($A\beta_{16-22}$) especially prone to supramolecular assembly to form fibrils and nanotubes.[7]

We recently began using macrocyclic β-sheet peptides containing the nonapeptide sequence QKLVFFAED ($A\beta_{15-23}$) as a model system with which to explore the structures and interactions of amyloid oligomers. We incorporated the $A\beta_{15-23}$ nonapeptide into a 66-membered ring macrocycle containing template and turn units that help enforce a β-sheet structure and block uncontrolled aggregation, and we studied the supramolecular assembly of the resulting macrocyclic β-sheet peptides **1** in the solid state by X-ray crystallography and in aqueous solution by NMR spectroscopy.[8,9] Macrocyclic β-sheets **1** contain an $A\beta_{15-23}$ peptide strand connected through two δ-linked ornithine turn units ($^{\delta}$Orn) to a template strand that contains two Hao amino acid tripeptide mimics.[10,11] In the solid

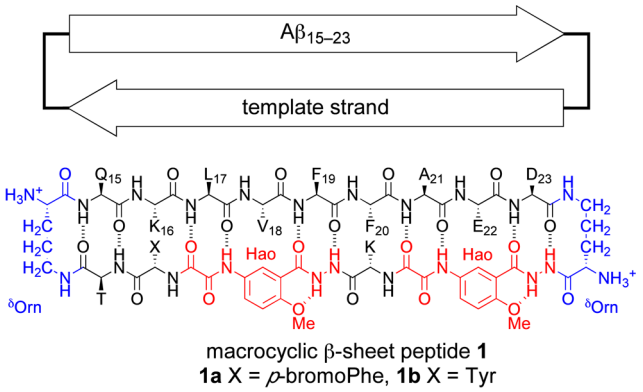

macrocyclic β-sheet peptide **1**
1a X = *p*-bromoPhe, **1b** X = Tyr

Received: June 6, 2014
Published: July 28, 2014

dx.doi.org/10.1021/ja505713y | J. Am. Chem. Soc. 2014, 136, 12682−12690

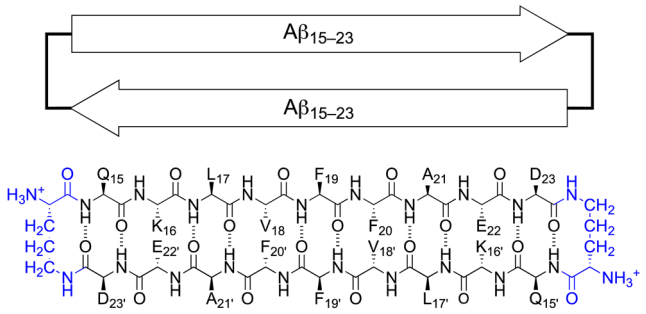

macrocyclic β-sheet peptide **2**

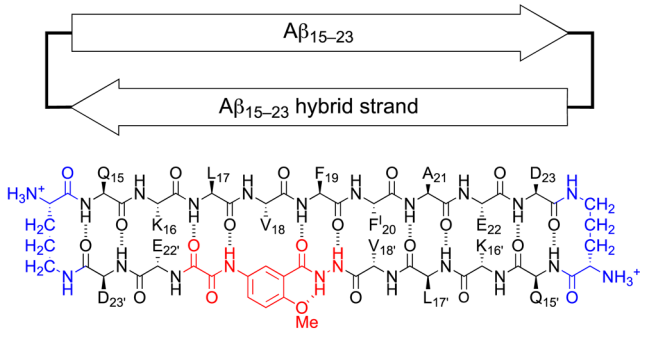

macrocyclic β-sheet peptide **3**

state, macrocyclic β-sheet peptide **1a** forms tetramers, dodecamers, and porelike assemblies of oligomers. In solution, macrocyclic β-sheets **1** form tetramers that differ in structure from those in the solid state. The differences between the solid-state and solution-state tetramers are important, because they reveal polymorphism among amyloid oligomers at atomic resolution and illustrate the importance of environment upon oligomer structure.

In the current study, we envisioned replacing the template strand with Aβ_{15-23} and determining the structures of the oligomers that form. Attempts to synthesize and study macrocyclic β-sheet peptide **2**, which embodies this concept, proved fruitless, yielding only an insoluble peptide hydrogel. Incorporating two full strands of Aβ_{15-23} into a macrocycle without a template designed to block aggregation appeared to give a peptide that was highly amyloidogenic. To reduce the amyloidogenicity of the macrocycle, we prepared macrocyclic β-sheet peptide **3**, which incorporates a single Hao amino acid in place of the $F_{19'}F_{20'}A_{21'}$ tripeptide segment of macrocyclic β-sheet **2**, to give an Aβ_{15-23} hybrid strand. To facilitate phase determination through single anomalous dispersion (SAD) phasing, we incorporated *p*-iodophenylalanine (F^I) in place of F_{20} in the Aβ_{15-23} peptide strand.

Here, we report the X-ray crystallographic structure of macrocyclic β-sheet **3**. We compare the solid-state supramolecular assembly to that of the oligomer observed in solution. We describe a new mode of assembly of Aβ_{15-23} in the solid state—a fibril-like assembly of oligomers—that resembles both fibrils and oligomers.

RESULTS

X-ray Crystallographic Structure of Macrocyclic β-Sheet 3. In the solid state, macrocyclic β-sheet **3** forms hydrogen-bonded dimers arranged in a herringbone fashion in offset layers that pack through hydrophobic interactions. The resulting supramolecular assembly differs substantially both from that which we have observed previously for macrocyclic β-sheets **1**[8,9] and that which others have previously observed for Aβ.

Macrocyclic β-sheet **3** readily formed crystals under sparse-matrix screening conditions with kits from Hampton Research. Crystals suitable for X-ray crystallography were grown from a 3.5 mg/mL solution with 0.1 M sodium citrate at pH 7.3, 0.1 M ammonium acetate, and 30% 2-methyl-2,4-pentanediol. Crystal diffraction data were collected on beamline 7-1 at the Stanford

Table 1. X-ray Crystallographic Data Collection and Refinement Statistics for Macrocyclic β-Sheet Peptide 3

Crystal parameters	
space group	*C*2
a, *b*, *c* (Å)	32.174, 62.852, 20.094
α, β, γ (deg)	90.00, 89.98, 90.00
molecules per asymmetric unit	2
Data collection	
synchrotron beamline	SSRL beamline 7−1
wavelength (Å)	1.00
resolution (Å)	17.56−1.75 (1.81−1.75)
total reflections[a]	14845 (1450)
unique reflections[a]	4060 (398)
completeness (%)[a]	99.2 (97.1)
multiplicity[a]	3.7 (3.6)
R_{merge} (%)[a,b]	3.6 (6.3)
$CC_{1/2}$ (%)[a]	99.8 (99.6)
CC* (%)[a]	100 (99.9)
$I/\sigma(I)$[a]	25.4 (13.4)
Refinement	
resolution (Å)	1.75
R_{work} (%)[c]	17.9
R_{free} (%)[d]	22.0
RMS bond lengths (Å)	0.010
RMS bond angles (deg)	1.52
ligands	2-methyl-2,4-pentanediol (2)
water	43
Ramachandran favored (%)	100
Ramachandran outliers (%)	0
Wilson *B*-factor (Å^2)	18.5
average *B*-factor (Å^2)	22.6
twinning	$-h$, $-k$, l (α = 0.49)

[a]Statistics for the highest resolution shell are shown in parentheses. [b]$R_{merge} = \sum|I - \langle I\rangle|/\sum I$. [c]$R_{work} = \sum|F_{obs} - F_{calc}|/\sum F_{obs}$. [d]$R_{free}$ was computed as R_{work} using a cross-validation set of 10% nonredundant data.

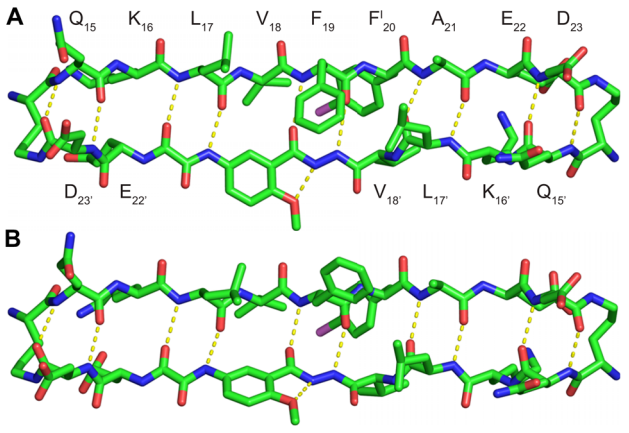

Figure 1. X-ray crystallographic structure of macrocyclic β-sheet peptide **3**. Two conformers (A and B) make up the asymmetric unit.

dx.doi.org/10.1021/ja505713y | J. Am. Chem. Soc. 2014, 136, 12682−12690

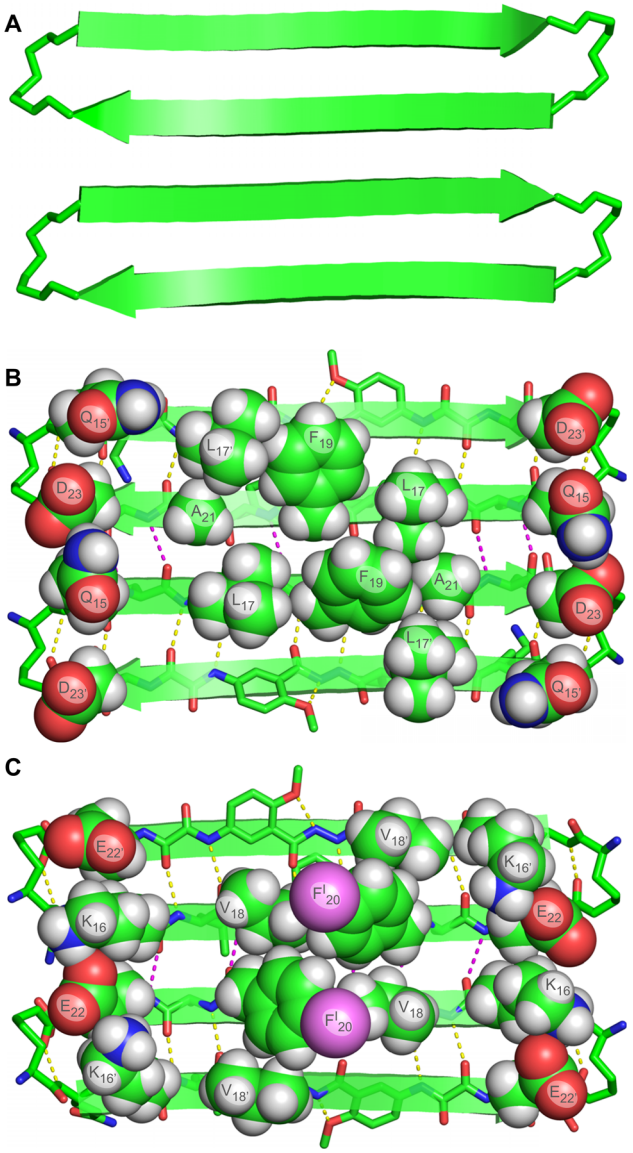

Figure 2. X-ray crystallographic structure of the hydrogen-bonded dimer of macrocyclic β-sheet peptide **3**. (A) Cartoon illustration of the hydrogen-bonded dimer. (B) The LFA face of the hydrogen-bonded dimer, bearing the side chains of residues Q_{15}, L_{17}, F_{19}, A_{21}, and D_{23} of the Aβ_{15-23} peptide strands and $Q_{15'}$, $L_{17'}$, and $D_{23'}$ of the Aβ_{15-23} hybrid strands. (C) The VF face of the hydrogen-bonded dimer, bearing the side chains of residues K_{16}, V_{18}, F^{I}_{20}, and E_{22} of the Aβ_{15-23} peptide strands and $K_{16'}$, $V_{18'}$, and $E_{22'}$ of the Aβ_{15-23} hybrid strands.

Synchotron Radiation Lightsource (SSRL) at 1.00 Å wavelength to 1.75 Å resolution. Data were integrated and scaled with XDS[12] and merged with Aimless.[13] Iodine locations were determined with HySS in the PHENIX software suite.[14] Initial density maps and phasing were generated with Autosol. Alternating rounds of manual rebuilding with Coot[15] and refinement with phenix.refine were performed. The structure was solved in the *C*2 space group with 49% pseudomerohedral twinning[16] to give a model with R_{free} = 22.0% and R_{work} = 17.9% (Table 1). The asymmetric unit contains two molecules of macrocyclic β-sheet **3** and two molecules of 2-methyl-2,4-pentanediol.

Macrocyclic β-sheet **3** crystallizes as a folded monomer in which the Aβ_{15-23} peptide strand and the Aβ_{15-23} hybrid strand form a hydrogen-bonded β-sheet. Two conformers of the macrocycle occur in the asymmetric unit, differing in rotamer

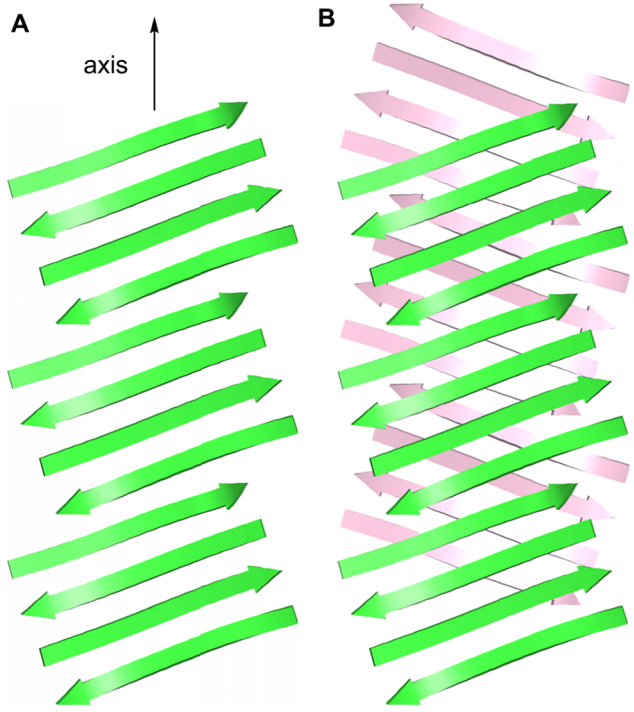

Figure 3. Assembly of hydrogen-bonded dimers in the X-ray crystallographic structure of macrocyclic β-sheet peptide **3**. (A) Extended β-sheet that runs the length of the crystal lattice. (B) Packing of the extended β-sheets to form a two-layered structure.

of F_{19} and tilt of the Hao amino acid. The conformers alternate in the crystal lattice, geared together through crystal packing. Figure 1 illustrates the structure of the two conformers of the macrocycle.

Macrocyclic β-sheet **3** forms a hydrogen-bonded dimer, in which the two conformers hydrogen bond to form a four-stranded antiparallel β-sheet. The Aβ_{15-23} peptide strands of the macrocycles make up the dimerization interface and are fully aligned, with residues 15−23 of one of the macrocycles paired with residues 23−15 of the other through eight hydrogen bonds. The side chains of residues Q_{15}, L_{17}, F_{19}, A_{21}, and D_{23} of the Aβ_{15-23} peptide strands and $Q_{15'}$, $L_{17'}$, and $D_{23'}$ of the Aβ_{15-23} hybrid strands decorate one of the surfaces of the four-stranded antiparallel β-sheet dimer; the side chains of residues K_{16}, V_{18}, F^{I}_{20}, and E_{22} of the Aβ_{15-23} peptide strands and $K_{16'}$, $V_{18'}$, and $E_{22'}$ of the Aβ_{15-23} hybrid strands decorate the other surface. Figure 2 illustrates the structure of the hydrogen-bonded dimer and the two surfaces. We term the two surfaces the LFA face and the VF face for the discussion of the higher-order supramolecular assembly of the dimers that follows.

The hydrogen-bonded dimers assemble to form an extended β-sheet that runs the length of the crystal lattice. The Aβ_{15-23} hybrid strands form the interfaces between the dimers. At the interfaces, the Aβ_{15-23} hybrid strands are not fully aligned, but rather are shifted out of alignment by two residues toward the C-termini. As a result of the shift in alignment, the β-strands comprising the β-sheets are not orthogonal to the axis formed by the extended β-sheet, but rather are rotated approximately 20° from orthogonality. The resulting assembly of the dimers resembles a herringbone pattern. Figure 3A illustrates the assembly of the hydrogen-bonded dimers.

The extended β-sheets formed by the hydrogen-bonded dimers pack through the VF faces to form a two-layered structure. The dimers comprising each layer do not overlap

dx.doi.org/10.1021/ja505713y | J. Am. Chem. Soc. 2014, 136, 12682−12690

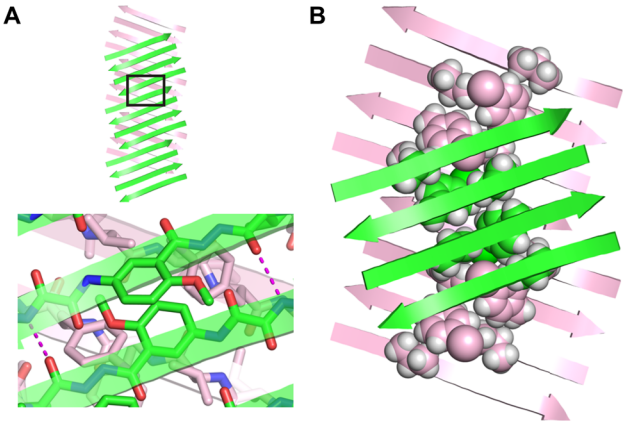

Figure 4. (A) Interaction between the Hao amino acids at the interface between dimers in the X-ray crystallographic structure of macrocyclic β-sheet peptide **3**. (B) Hydrophobic core formed by the side chains of the V_{18}, F^{I}_{20}, and $V_{18'}$ residues, between the layers of the extended β-sheets in the X-ray crystallographic structure of macrocyclic β-sheet **3**.

directly. Instead, each dimer in one layer sits over the interface between two dimers in the opposite layer. Figure 3B illustrates the packing of the two layers.

The Hao amino acids come together at the interface between the hydrogen-bonded dimers, tilting alternately upward and downward and stacking to accommodate hydrogen-bonding interactions between the Aβ_{15-23} hybrid strands.[17] Figure 4A illustrates the interaction between the Hao amino acids at the interface. The side chains of the V_{18}, F^{I}_{20}, and $V_{18'}$ residues create a hydrophobic core that runs along the axis formed by the extended β-sheet. Figure 4B illustrates the structure of the hydrophobic core. The stacked Hao amino acids and the iodine of F^{I}_{20} help fill the void created by the absence of $F_{20'}$ in the Aβ_{15-23} hybrid strand. The 2-methyl-2,4-pentanediol solvent that crystallizes with macrocyclic β-sheet **3** packs alongside the hydrophobic core and further stabilizes the two-layered structure through additional hydrophobic interactions.

Solution-State Studies of Macrocyclic β-Sheets 3–6. In aqueous solution, macrocyclic β-sheet **3** forms discrete tetramers comprising a sandwich formed by two hydrogen-bonded dimers. The solution-state tetramer is similar in structure to that which we have previously observed for macrocyclic β-sheets **1**.[9] The dimer subunits form through hydrogen bonding between the Aβ_{15-23} peptide strands, with the β-strands shifted out of alignment by two residues toward the C-termini. The dimer subunits assemble to form the tetramer through hydrophobic interactions between the LFA faces.

We studied the folding and supramolecular assembly of macrocyclic β-sheet **3** and homologues **4**, **5**, and **6** by ^{1}H NMR NOESY and DOSY experiments on the trifluoroacetate (TFA) salts in D_2O solution. Macrocyclic β-sheet **4** is a homologue of macrocyclic β-sheet **3** with phenylalanine in place of *p*-iodophenylalanine in the Aβ_{15-23} peptide strand (F_{20} in place of F^{I}_{20}). Macrocyclic β-sheet **5** is a double mutant in which the hydrophobic residues V_{18} and F_{20} in the Aβ_{15-23} peptide strand are rendered more hydrophilic by hydroxylation: V_{18} is replaced by threonine and F_{20} is replaced by tyrosine (V_{18}T,F_{20}Y). Macrocyclic β-sheet **6** is another double mutant in which the hydrophobic residues F_{19} and A_{21} in the Aβ_{15-23} peptide strand are rendered more hydrophilic by hydroxylation: F_{19} is replaced by tyrosine and A_{21} is replaced by serine (F_{19}Y,A_{21}S).

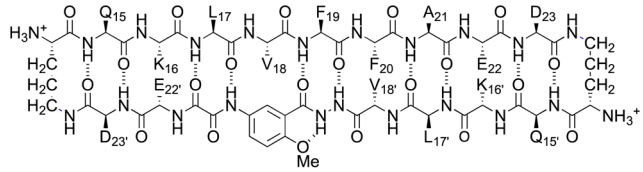
macrocyclic β-sheet peptide **4**

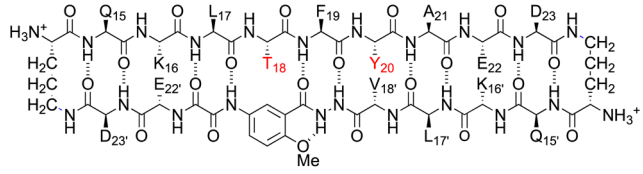
macrocyclic β-sheet peptide **5**

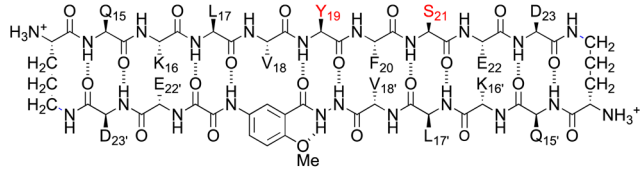
macrocyclic β-sheet peptide **6**

Table 2. Key NOEs Observed for Peptides 3, 4, and 5[a]

peptide	K_{16}—$E_{22'}$ [b]	X_{18}—Hao$_6$	X_{20}—$V_{18'}$	$E_{22'}$—$K_{16'}$ [b]	L_{17}—D_{23} [b]	F_{19}—A_{21} [b]
3	obs[c]	obs	obs	–[c,d]	obs	–[d]
4	obs	obs	obs	obs	obs	obs
5	obs	obs	obs	obs	obs	obs

[a] 500 MHz NOESY spectra at 2.0 mM in D_2O at 298 K. [b] Assignments of K_{16} vs $K_{16'}$, L_{17} vs $L_{17'}$, E_{22} vs $E_{22'}$, and D_{23} vs $D_{23'}$ are inferred from the observed pattern of NOEs. [c] Assignment of K_{16}—$E_{22'}$ vs E_{22}—$K_{16'}$ is arbitrary. [d] NOEs not observed due to overlap of the resonances. (**3**: X_{18} = V, X_{20} = F^{I}; **4**: X_{18} = V, X_{20} = F; **5**: X_{18} = T, X_{20} = Y)

^{1}H NMR studies establish that macrocyclic β-sheets **3**, **4**, and **5** form tetramers comprising hydrogen-bonded dimer subunits at low millimolar concentrations.[18] The three macrocycles exhibit ^{1}H NMR spectra with similar features (Figure S1). All three macrocycles show downfield shifting of the α-protons characteristic of β-sheet structure, magnetic anisotropy of the δ-linked ornithine *pro-R* and *pro-S* δ-protons characteristic of well-defined turn structures,[10] and upfield shifting of the F_{19} aromatic resonances characteristic of tertiary and quaternary structure (Figures S1–S2, Table S1).[19] In contrast, macrocyclic β-sheet **6** is monomeric at low millimolar concentrations and is less well folded than macrocyclic β-sheets **3**–**5**, exhibiting less downfield shifting of the α-protons and less magnetic anisotropy of the δ-linked ornithine pro-R and pro-S δ-protons (Figure S1).[20]

In the NOESY spectra, macrocyclic β-sheets **3**, **4**, and **5** exhibit a rich array of NOE crosspeaks associated with folding and dimerization (Figures S3–S5). The macrocycles exhibit key NOEs between α-protons associated with folding: K_{16} and $E_{22'}$; V_{18} or T_{18} and the proton at the 6-position of the Hao residue; F^{I}_{20}, F_{20}, or Y_{20} and $V_{18'}$; and E_{22} and $K_{16'}$. The macrocycles also exhibit key NOEs between α-protons associated with dimerization: L_{17} and D_{23}; and F_{19} and A_{21}. Table 2 summarizes the key NOEs observed for each macrocycle; Figure 5 illustrates the structures of the dimers.

DOSY studies show that the hydrogen-bonded dimers are subunits of tetramers, which are the stable species in aqueous solution.[18,19,21,22] In the DOSY spectra macrocyclic β-sheets **3**,

dx.doi.org/10.1021/ja505713y | J. Am. Chem. Soc. 2014, 136, 12682–12690

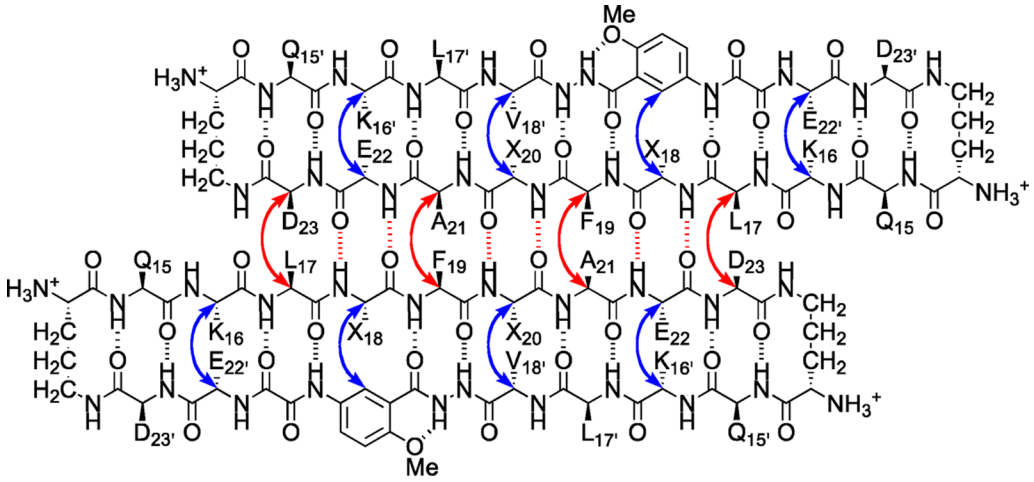

Figure 5. Hydrogen-bonded dimers formed by macrocyclic β-sheet peptides **3**–**5** in aqueous solution. Key NOEs associated with dimerization and folding are shown with red and blue arrows. (**3**: X_{18} = V, X_{20} = F^I; **4**: X_{18} = V, X_{20} = F; **5**: X_{18} = T, X_{20} = Y).

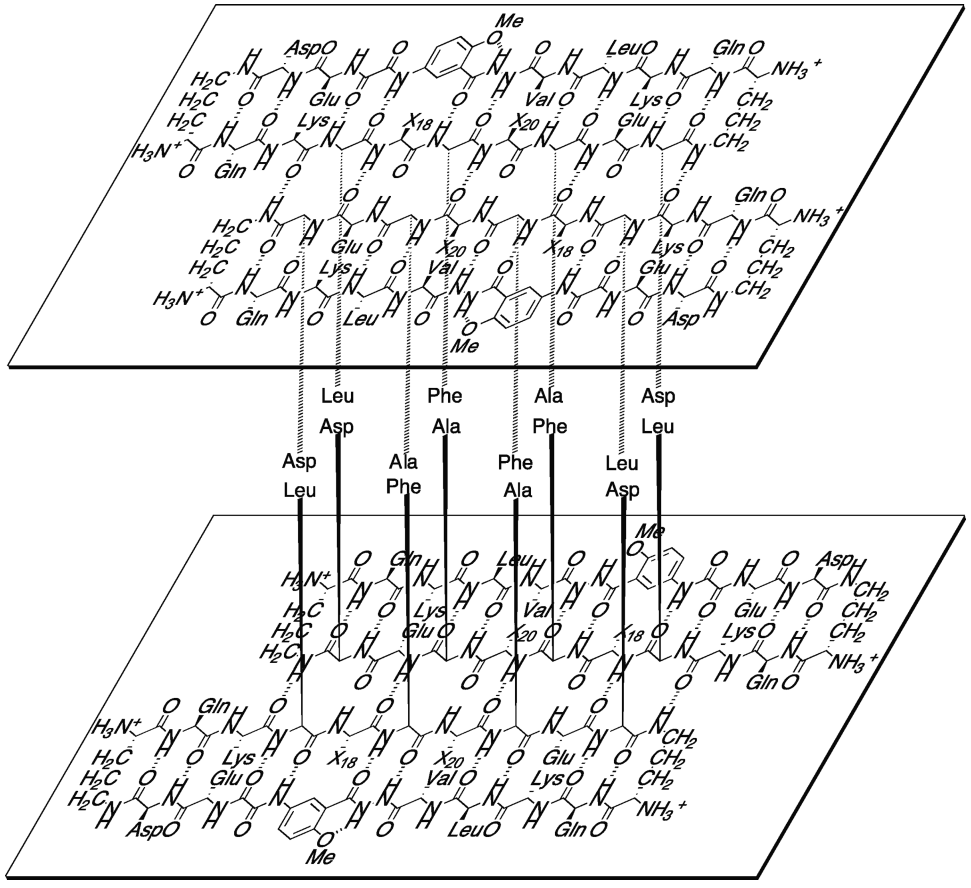

Figure 6. Illustration of the tetramer formed by macrocyclic β-sheet peptides **3**–**5** in aqueous solution. The tetramer forms as a sandwich-like assembly of two hydrogen-bonded dimers, sandwiched through the LFA faces (**3**: X_{18} = V, X_{20} = F^I; **4**: X_{18} = V, X_{20} = F; **5**: X_{18} = T, X_{20} = Y).

4, and **5** exhibit diffusion coefficients of 10.1–10.7 × 10^{-7} cm^2/s (Table 3). These values are comparable to those that we have observed previously for similar tetramers and are 0.58–0.61 times smaller than that of macrocyclic β-sheet **6**, which is monomeric.[9,23,24]

The tetramer forms as a sandwich of hydrogen-bonded dimers. It is sandwiched through the hydrophobic face that displays L_{17}, F_{19}, and A_{21}, and these residues help create the hydrophobic core of the tetramer (Figure 6). When F_{19} and A_{21} are rendered hydrophilic by hydroxylation in macrocyclic

Table 3. Diffusion Coefficients (D) of Peptides 3–6 at 2.0 mM in D_2O at 298 K

peptide	$MW_{monomer}$[a] (Da)	$MW_{tetramer}$[a] (Da)	D (10^{-7} cm^2/s)	oligomer state
3	2380	9522	10.1	tetramer
4	2254	9018	10.3	tetramer
5	2272	9090	10.7	tetramer
6	2286	NA	17.4	monomer

[a]Molecular weight calculated for the neutral (uncharged) macrocycle.

dx.doi.org/10.1021/ja505713y | J. Am. Chem. Soc. 2014, 136, 12682–12690

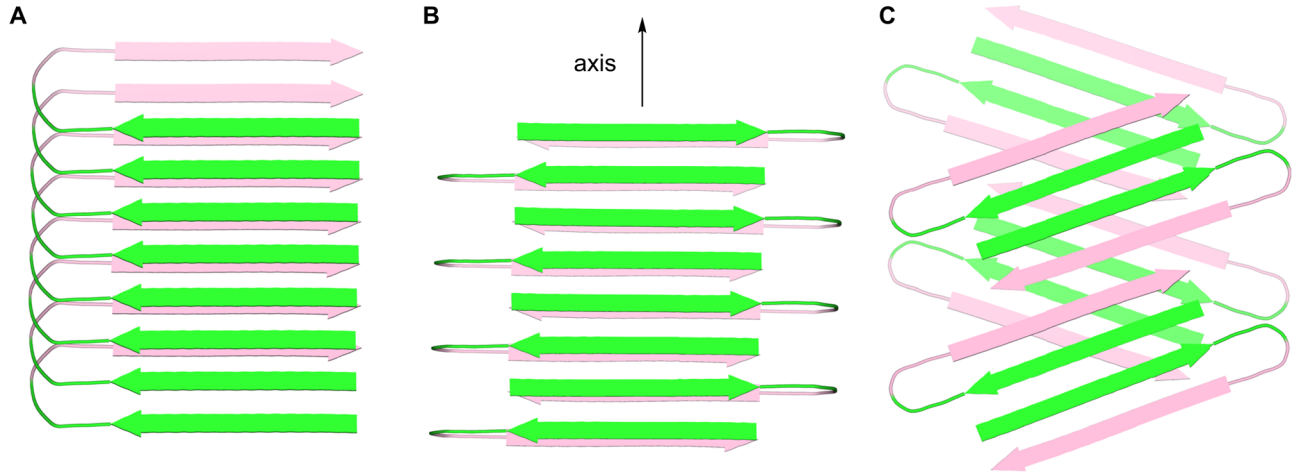

Figure 7. Cartoon representations of fibrils formed by Aβ. (A) Parallel β-sheet fibril composed of U-shaped turns in a staggered arrangement, observed for Aβ_{1-40}.[2c] (B) Antiparallel β-sheet fibril composed of U-shaped turns, observed for the Iowa mutant Aβ_{1-40}.[27] (C) Fibril-like assembly of oligomers composed of β-hairpins, that we propose from the X-ray crystallographic structure of macrocyclic β-sheet peptide **3**. The green and pink colors represent the central and C-terminal regions of Aβ.

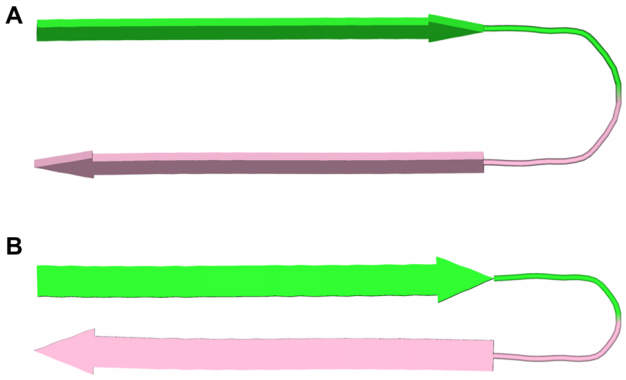

Figure 8. Cartoon representations of U-shaped turns (A) and β-hairpins (B) composed of Aβ. In the U-shaped turns, the faces of the β-strands pack together.[2c,27] In the proposed β-hairpins, the edges of the β-strands hydrogen bond together. The green and pink colors represent the central and C-terminal regions of Aβ.

β-sheet **6**, the hydrophobic core cannot form and the tetramer is disrupted.[9] In contrast, when V_{18} and F_{20} are rendered hydrophilic by hydroxylation in macrocyclic β-sheet **5**, the hydrophobic core is unaffected and the tetramer is not disrupted.

DISCUSSION

The extended layered β-sheet formed by the hydrogen-bonded dimers of **3** (Figure 3B) resembles the structures of amyloid fibrils.[25,26] Amyloid fibrils consist of extended β-sheets composed of networks of hydrogen-bonded β-strands running the length of the fibril axis and laminated in pairs through hydrophobic interactions to form two-layered assemblies.[2] In the fibrils formed by Aβ_{1-40}, the hydrophobic central and C-terminal regions of the peptide assemble to form extended β-sheets that run the length of the fibril axis. The β-strands comprising the β-sheets are roughly orthogonal (90°) to the fibril axis. The molecules of Aβ form U-shaped turns, and the hydrophobic central and C-terminal β-strands pack in a face-to-face fashion through hydrophobic interactions. The resulting two-layered β-sheets make up the basic fibril structure, further assembling to form four-layered or triangular fibrils consisting of two or three of these subunits. Although most of the structures reported for Aβ_{1-40} fibrils involve parallel β-sheets, antiparallel β-sheets have been reported for Iowa mutant β-amyloid fibrils.[27] Figure 7A,B illustrates the structures of the parallel and antiparallel two-layered β-sheets reported for Aβ_{1-40}. Figure 8A illustrates the structure of the component U-shaped turns that make up these two-layered assemblies.

The assembly formed by the hydrogen-bonded dimers of **3** (Figure 3B) differs notably from amyloid fibrils in that it is composed of discrete oligomeric subunits. While the two-layered β-sheets of the Aβ_{1-40} fibrils contain no subunit larger than the monomer, the fibril-like assemblies formed by macrocyclic β-sheet **3** are composed of oligomers consisting of two β-hairpin-like macrocycles, hydrogen bonded to form a four-stranded antiparallel β-sheet.

The X-ray crystallographic structure of the fibril-like assembly of oligomers formed by macrocyclic β-sheet **3** suggests that alternative fibril assemblies of Aβ_{1-40} or Aβ_{1-42} might also be possible.[25,26] In a fibril-like assembly of oligomers formed by full-length Aβ, the hydrophobic central and C-terminal regions of the peptide could hydrogen bond to form a β-hairpin.[28] The β-hairpins could then further assemble to form layered β-sheets through edge-to-edge hydrogen bonding and face-to-face hydrophobic interactions. In this assembly, the β-strands comprising the β-sheets are not orthogonal to the fibril axis, but rather are rotated approximately 20° from orthogonality. To compensate for this rotation, the β-sheets must shift registration by two residues for every two β-hairpins. Figure 7C illustrates a structure of this fibril-like assembly of oligomers; Figure 8B illustrates the structure of the component β-hairpins.

The solid-state and solution-state structures of macrocyclic β-sheets **3**–**5** show that Aβ_{15-23} can form both aligned and shifted antiparallel β-sheets. In the X-ray crystallographic structure of macrocyclic β-sheet **3**, the Aβ_{15-23} peptide strand forms an aligned β-sheet, while the Aβ_{15-23} hybrid strand forms a shifted β-sheet. In the solution-state structure of macrocyclic β-sheets **3**–**5**, the Aβ_{15-23} peptide strand forms a shifted β-sheet. Figure 9 illustrates these modes of supramolecular assembly.

We have previously observed both aligned and shifted antiparallel β-sheets involving Aβ_{15-23} in the solid-state and solution-state structures of macrocyclic β-sheets **1**. In the

dx.doi.org/10.1021/ja505713y | J. Am. Chem. Soc. 2014, 136, 12682–12690

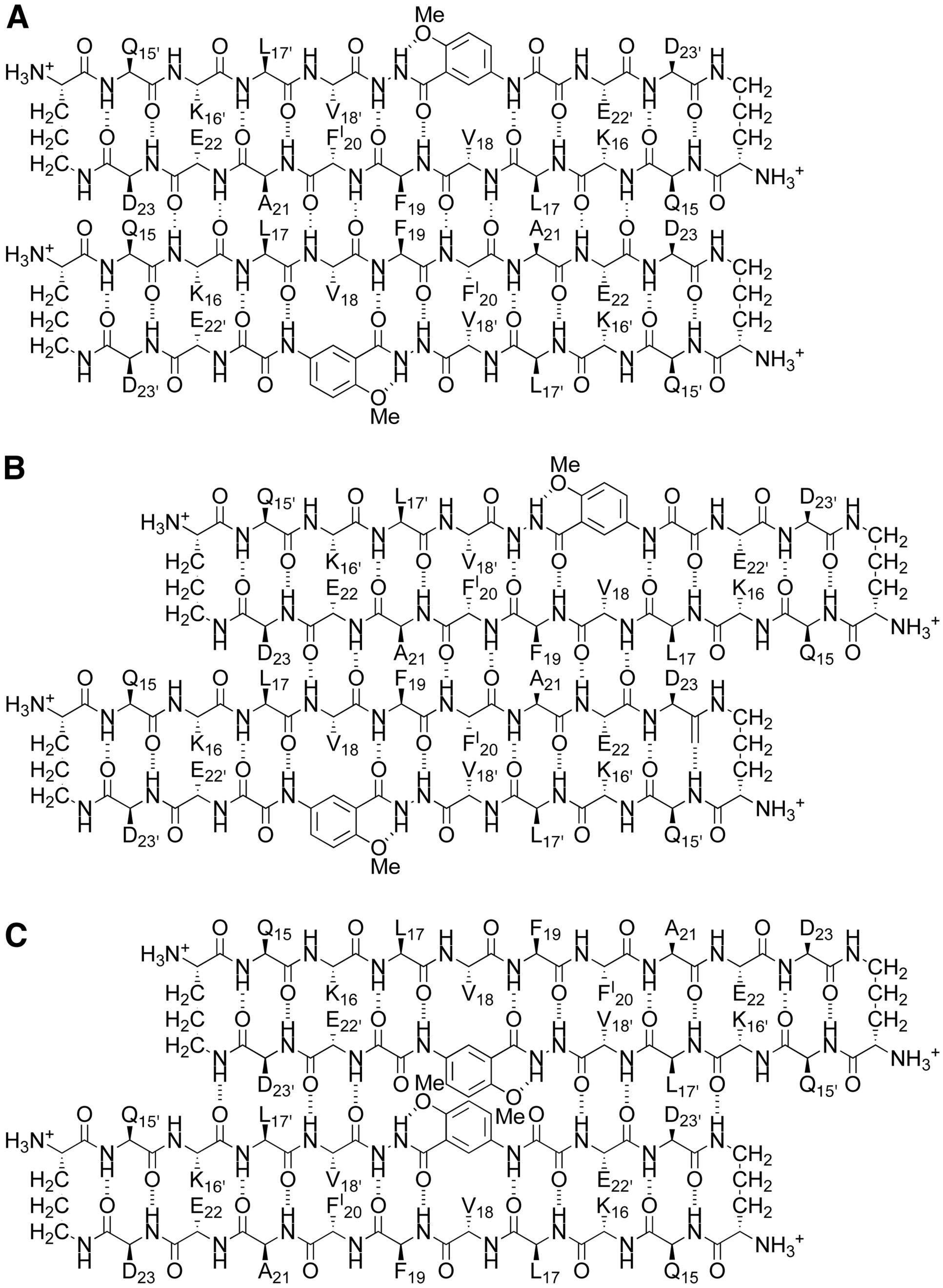

Figure 9. Interfaces between Aβ_{15-23} observed in the solid state and in solution. (A) Interface between monomer subunits within the dimer of macrocyclic β-sheet peptide **3** in the solid state. (B) Interface between monomer subunits within the dimer of macrocyclic β-sheet **3** in aqueous solution. (C) Interface between the dimers of macrocyclic β-sheet **3** in the solid state. In (A) and (B) the interface occurs between the Aβ_{15-23} peptide strands; in (C) the interface occurs between the Aβ_{15-23} hybrid strands.

solid state, macrocyclic β-sheet **1a** forms tetramers consisting of two hydrogen-bonded dimers sandwiched through the VF faces (Figure 10A).[8] In these hydrogen-bonded dimers, the Aβ_{15-23} peptide strands are fully aligned. In aqueous solution, macrocyclic β-sheets **1a** and **1b** form tetramers consisting of two hydrogen-bonded dimers sandwiched through the LFA faces (Figure 10B).[9] In these hydrogen-bonded dimers, the Aβ_{15-23} peptide strands are shifted out of alignment by two residues toward the C-termini. The fibril-like assembly of oligomers formed by macrocyclic β-sheet **3** differs from the solid-state and solution-state structures of macrocyclic β-sheets **1**, in that it does not contain discrete tetramers. Instead, each dimer subunit overlaps with two dimers in the opposing layer (Figure 10C).

It is easy to imagine a mechanism, similar to crystallization, by which the fibril-like assemblies of oligomers catalyze oligomer formation.[29] During crystal growth, the fibril-like oligomers of macrocyclic β-sheet **3** shown in Figure 3B must elongate by adding monomer subunits either one at a time or in small groups from tetramers or oligomers present in solution. A similar mechanism of growth can be hypothesized for the fibril-like assemblies of oligomers that we propose for full-length Aβ in Figure 7C, in which the exposed hydrogen-bonding edges and hydrophobic surfaces serve as a template that promotes the

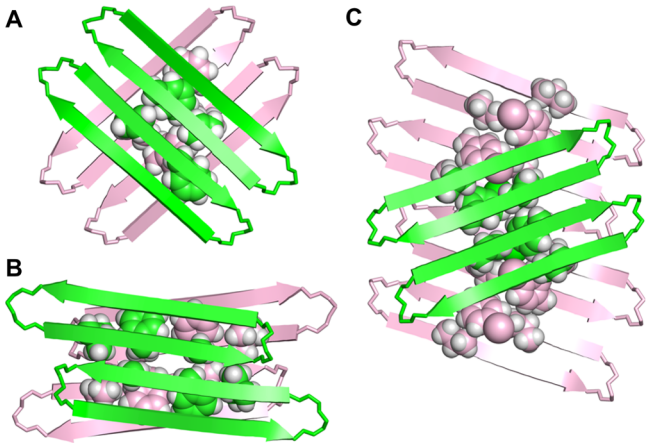

Figure 10. Supramolecular assemblies of macrocyclic β-sheet peptides derived from Aβ_{15-23}. (A) Tetramer of **1a** observed in the solid state (PDB: 4IVH).[8] (B) Tetramer of **1b** (and **1a**) observed in aqueous solution.[9] (C) Fibril-like assembly of dimers of **3** observed in the solid state.

addition and folding of monomeric Aβ. The fibril-like assembly of oligomers can then serve as a reservoir of oligomers, dissociating organized dimers, tetramers, or other small homogeneous assemblies of soluble toxic amyloid oligomers. Such mechanisms for oligomer replication have been seen and discussed previously but have not been observed at atomic resolution.[30] The X-ray crystallographic structure of macrocyclic β-sheet **3** may thus provide a window at atomic resolution into a prion-like mechanism of amyloid oligomer propagation.

CONCLUSION

The X-ray crystallographic structure of macrocyclic β-sheet **3** provides new insights into the supramolecular assembly of peptides from β-amyloid, revealing a fibril-like assembly of hydrogen-bonded dimers. The dimers repeat along the fibril axis, to form an extended β-sheet, like in conventional amyloid fibrils. Unlike conventional amyloid fibrils, the β-strands comprising the β-sheets are rotated approximately 20° from orthogonality to the fibril axis, and a two-residue shift in alignment of the β-strands occurs at the juncture between the dimers. The β-sheets are layered and laminated through hydrophobic interactions. The dimers are not layered directly over each other, but rather are offset by two strands. As a result, the fibril-like assembly of dimers is not composed of discrete tetramers.

The fibril-like assembly of oligomers formed by macrocyclic β-sheet **3** offers the intriguing possibility that full-length Aβ may also be able to form similar assemblies, perhaps consisting of β-hairpins formed by the amyloidogenic central and C-terminal regions of Aβ. This model further suggests the provocative hypothesis that fibril-like assemblies of Aβ oligomers might catalyze Aβ oligomer formation and replication.

ASSOCIATED CONTENT

Supporting Information

NMR spectra, mass spectra, and HPLC traces for macrocyclic β-sheet peptides **3**–**6**. Crystallographic data in CIF and PDB format for macrocyclic β-sheet **3**. The crystal structure of macrocyclic β-sheet **3** was deposited into the Protein Data Bank (PDB) with PDB code 4Q8D. This material is available free of charge via the Internet at http://pubs.acs.org.

AUTHOR INFORMATION

Corresponding Author

jsnowick@uci.edu

Notes

The authors declare no competing financial interest.

ACKNOWLEDGMENTS

We thank the National Institutes of Health for grant support (5R01GM097562). J.D.P. thanks Dr. Nicholas Chim for helpful discussion of structure refinement. K.H.C. thanks Vertex Pharmaceuticals for support through the Vertex Scholars program. Use of the Stanford Synchrotron Radiation Lightsource, SLAC National Accelerator Laboratory, is supported by the U.S. Department of Energy, Office of Science, Office of Basic Energy Sciences under contract no. DE-AC02-76SF00515. The SSRL Structural Molecular Biology Program is supported by the DOE Office of Biological and Environmental Research and by the National Institutes of Health, National Institute of General Medical Sciences (including P41GM103393).

REFERENCES

(1) (a) Hamley, I. W. *Chem. Rev.* **2012**, *112*, 5147−5192. (b) Benilova, I.; Karran, E.; De Strooper, B. *Nat. Neurosci.* **2012**, *15*, 349−357. (c) Querfurth, H. W.; LaFerla, F. H. N *N. Engl. J. Med.* **2010**, *362*, 329−344. (d) Larson, M. E.; Lesné, S. E. *J. Neurochem.* **2012**, *192* (Suppl. 1), 125−139. (e) Fändrich, M. *J. Mol. Biol.* **2012**, *421*, 427−440.

(2) (a) Benzinger, T. L.; Gregory, D. M.; Burkoth, T. S.; Miller-Auer, H.; Lynn, D. G.; Botto, R. E.; Meredith, S. C. *Proc. Natl. Acad. Sci. U.S.A.* **1998**, *95*, 13407−13412. (b) Lührs, T.; Ritter, C.; Adrian, M.; Riek-Loher, D.; Bohrmann, B.; Döbeli, H.; Schubert, D.; Riek, R. *Proc. Natl. Acad. Sci. U.S.A.* **2005**, *102*, 17342−17347. (c) Petkova, A. T.; Yau, W.-M.; Tycko, R. *Biochemistry* **2006**, *45*, 498−512. (d) Paravastu, A. K.; Leapman, R. D.; Yau, W.-M.; Tycko, R. *Proc. Natl. Acad. Sci. U.S.A.* **2008**, *105*, 18349−18354. (e) McDonald, M.; Box, H.; Bian, W.; Kendall, A.; Tycko, R.; Stubbs, G. *J. Mol. Biol.* **2012**, *423*, 454−461.

(3) (a) Yu, L.; Edalji, R.; Harlan, J. E.; Holzman, T. F.; Lopez, A. P.; Labkovsky, B.; Hillen, H.; Barghorn, S.; Ebert, U.; Richardson, P. L.; Miesbauer, L.; Solomon, L.; Bartley, D.; Walter, K.; Johnson, R. W.; Hajduk, P. J.; Olejniczak, E. T. *Biochemistry* **2009**, *48*, 1870−1877. (b) Cerf, E.; Sarroukh, R.; Tamamizu-Kato, S.; Breydo, L.; Derclaye, S.; Dufrêne, Y. V.; Narayanaswami, V.; Goormaghtigh, E.; Ruysschaert, J.-M.; Raussens, V. *Biochem. J.* **2009**, *421*, 415−423. (c) Chimon, S.; Shaibat, M. A.; Jones, C. R.; Calero, D. C.; Aizezi, B.; Ishii, Y. *Nat. Struc. Mol. Bio.* **2010**, *14*, 1157−1164. (d) Streltsov, V. A.; Varghese, J. N.; Masters, C. L.; Nuttall, S. D. *J. Neurosci.* **2011**, *31*, 1419−1426.

(4) (a) Ma, B.; Nussinov. *Proc. Natl. Acad. Sci. U.S.A.* **2002**, *99*, 14126−14131. (b) Tarus, B.; Straub, J. E.; Thirumalai, D. *J. Mol. Biol.* **2005**, *345*, 1141−1156. (c) Miller, Y.; Ma, B.; Nussinov, R. *Biophys. J.* **2009**, *97*, 1168−1177. (d) Ahmed, M.; Davis, J.; Aucoin, D.; Sato, T.; Ahuja, S.; Aimoto, S.; Elliott, J. I.; van Nostrand, W. E.; Smith, S. O. *Nat. Struct. Mol. Biol.* **2010**, *17*, 561−567.

(5) (a) Hilbich, C.; Kisters-Woike, B.; Reed, J.; Masters, C. L.; Beyreuther, K. *J. Mol. Biol.* **1992**, *228*, 460−473. (b) Wood, S. J.; Wetzel, R.; Martin, J. D.; Hurle, M. R. *Biochemistry* **1995**, *34*, 724−730. (c) Tjernberg, L. O.; Callaway, D. J. E.; Tjernberg, A.; Hahne, S.; Lilliehöök, C.; Terenius, L.; Thyberg, J.; Nordstedt, C. *J. Biol. Chem.* **1999**, *274*, 12619−12625.

(6) (a) Tjernberg, L. O.; Näslund, J.; Lindqvist, F.; Johansson, J.; Karlström, A. R.; Thyberg, J.; Terenius, L.; Nordstedt, C. *J. Biol. Chem.* **1996**, *271*, 8545−8548. (b) Tjernberg, L. O.; Lilliehöök, C.; Callaway, D. J. E.; Näslund, J.; Hahne, S.; Thyberg, J.; Terenius, L.; Nordstedt, C. *J. Biol. Chem.* **1997**, *272*, 12601−12605. (c) Soto, C.; Kindy, M. S.; Baumann, M.; Frangione, B. *Biochem. Biophys. Res. Commun.* **1996**,

226, 672−680. (d) Findeis, M. A.; Musso, G. M.; Arico-Muendel, C. C.; Benjamin, H. W.; Hundal, A. M.; Lee, J. J.; Chin, J.; Kelley, M.; Wakefield, J.; Hayward, N. J.; Molineaux, S. M. *Biochemistry* **1999**, *38*, 6791−6800.

(7) (a) Balbach, J. J.; Ishii, Y.; Antzutkin, O. N.; Leapman, R. D.; Rizzo, N. W.; Dyda, F.; Reed, J.; Tycko, R. *Biochemistry* **2000**, *39*, 13748−13759. (b) Ishii, Y.; Tycko, R. J. *Am. Chem. Soc.* **2003**, *125*, 6606−6607. (c) Klimov, D.; Thirumalai, D. *Structure* **2003**, *11*, 295−307. (d) Petkova, A. T.; Buntkowsky, G.; Dyda, F.; Leapman, R. D.; Yau, W. M.; Tycko, R. *J. Mol. Biol.* **2004**, *335*, 247−260. (e) Lu, K.; Jacob, J.; Thiyagarajan, P.; Conticello, V. P.; Lynn, D. G. *J. Am. Chem. Soc.* **2003**, *125*, 6391−6393. (f) Mehta, A. K.; Lu, K.; Childers, W. S.; Liang, Y.; Dublin, S. N.; Dong, J.; Snyder, J. P.; Pingali, S. V.; Thiyagarajan, P.; Lynn, D. G. *J. Am. Chem. Soc.* **2008**, *130*, 9829−9835. (g) Liang, Y.; Pingali, S. V.; Jogalekar, A. S.; Snyder, J. P.; Thiyagarajan, P.; Lynn, D. G. *Biochemistry* **2008**, *47*, 10018−10026. (h) Senguen, F. T.; Lee, N. R.; Gu, X.; Ryan, D. M.; Doran, T. M.; Anderson, E. A.; Nilsson, B. L. *Mol. BioSyst.* **2011**, *7*, 486−496. (i) Senguen, F. T.; Doran, T. M.; Anderson, E. A.; Nilsson, B. L. *Mol. BioSyst.* **2011**, *7*, 497−510. (j) Colletier, J.-P.; Laganowsky, A.; Landau, M.; Zhao, M.; Soriaga, A. B.; Goldschmidt, L.; Flot, D.; Cascio, D.; Sawaya, M. R.; Eisenberg, D. *Proc. Natl. Acad. Sci. U.S.A.* **2011**, *108*, 16938−16943. (k) Cheng, P.-N.; Liu, C.; Zhao, M.; Eisenberg, D.; Nowick, J. S. *Nat. Chem.* **2012**, *4*, 927−933.

(8) Pham, J. D.; Chim, N.; Goulding, C. W.; Nowick, J. S. *J. Am. Chem. Soc.* **2013**, *135*, 12460−12467.

(9) Pham, J. D.; Demeler, B.; Nowick, J. S. *J. Am. Chem. Soc.* **2014**, *136*, 5432−5442.

(10) Nowick, J. S.; Brower, J. O. *J. Am. Chem. Soc.* **2003**, *125*, 876−877.

(11) Nowick, J. S.; Chung, D. M.; Maitra, K.; Maitra, S.; Stigers, K. D.; Sun, Y. J. *J. Am. Chem. Soc.* **2000**, *122*, 7654−7661.

(12) Kabsch, W. *Acta Crystallogr., Sect. D: Biol. Crystallogr.* **2010**, *66*, 125−132.

(13) (a) Evans, P. *Acta Crystallogr., Sect. D: Biol. Crystallogr.* **2006**, *62*, 72−82. (b) Evans, P. R.; Murshudov, G. N. *Acta Crystallogr., Sect. D: Biol. Crystallogr.* **2013**, *69*, 1204−1214.

(14) (a) Grosse-Kunstleve, R. W.; Adams, P. D. *Acta Crystallogr., Sect. D: Biol. Crystallogr.* **2003**, *59*, 1966−1973. (b) Adams, P. D.; Afonine, P. V.; Bunkoczi, G.; Chen, V. B.; Davis, I. W.; Echols, N.; Headd, J. J.; Hung, L. W.; Kapral, G. J.; Grosse-Kunstleve, R. W.; McCoy, A. J.; Moriarty, N. W.; Oeffner, R.; Read, R. J.; Richardson, D. C.; Richardson, J. S.; Terwilliger, T. C.; Zwart, P. H. *Acta Crystallogr., Sect. D: Biol. Crystallogr.* **2010**, *66*, 213−221.

(15) Emsley, P.; Lohkamp, B.; Scott, W. G.; Cowtan, K. *Acta Crystallogr., Sect. D: Biol. Crystallogr.* **2010**, *66*, 486−501.

(16) Larsen, N. A.; Heine, A.; de Prada, P.; Redwan, E.-R.; Yeates, T. O.; Landry, D. W.; Wilson, I. A. *Acta Crystallogr., Sect. D: Biol. Crystallogr.* **2002**, *58*, 2055−2059.

(17) We were surprised to see this type of interaction between the Hao amino acids in the Aβ_{15-23} hybrid strands, having previously described it as "forbidden" (Figure 2B of reference 25b). It thus appears that the Hao amino acid disfavors, but does not completely preclude, the formation of extended networks of β-sheets.

(18) Macrocyclic β-sheet **5** shows predominantly or wholly the tetramer in the ^{1}H NMR spectrum at concentrations as low as 0.1 mM in D_2O at 298 K.

(19) The ^{1}H NMR spectra of macrocyclic β-sheets **3** and **4** are broader than that of **5**, suggesting that while the tetramers predominate for all of these peptides, the tetramers formed by the more hydrophobic peptides **3** and **4** may participate in minor equilibria with additional tetramers that differ in structure or oligomers that differ in molecularity.

(20) Macrocyclic β-sheet **6** shows only monomer in the ^{1}H NMR spectrum at 2.0 mM in D_2O at 298 K but shows resonances for both monomer and oligomer at 8.0 mM.

(21) (a) Berger, S.; Braun, S. *200 and More NMR Experiments: A Practical Course*; Wiley-VCH: Weinheim, 2004; pp 515−517. (b) Findeisen, M.; Berger, S. *50 and More Essential NMR Experiments*; Wiley-VCH: Weinheim, 2012; pp 163−166.

(22) (a) Altieri, A. S.; Hinton, D. P.; Byrd, R. A. *J. Am. Chem. Soc.* **1995**, *117*, 7566−7567. (b) Johnson, C. S. *Progr. NMR Spectrosc.* **1999**, *34*, 203−256. (c) Yao, S.; Howlett, G. J.; Norton, R. S. *J. Biomol. NMR* **2000**, *16*, 109−119. (d) Cohen, Y.; Avram, L.; Frish, L. *Angew. Chem., Int. Ed.* **2005**, *44*, 520−554. (e) Cohen, Y.; Avram, L.; Evan-Salem, T.; Slovak, S.; Shemesh, N.; Frish, L. In *Analytical Methods in Supramolecular Chemistry*, 2nd ed.; Schalley, C. A., Ed; Wiley-VCH: Weinheim, 2012; 197−285.

(23) Khakshoor, O.; Demeler, B.; Nowick, J. S. *J. Am. Chem. Soc.* **2007**, *129*, 5558−5569.

(24) (a) Polson, A. *J. Phys. Colloid Chem.* **1950**, *54*, 649−652. (b) Teller, D. C.; Swanson, E.; DeHaen, C. *Methods Enzymol.* **1979**, *61*, 103−124.

(25) Fibril-like assemblies of oligomers have been proposed and observed previously for other macrocyclic β-sheet peptides containing amyloidogenic peptide sequences: (a) Liu, C.; Sawaya, M. R.; Cheng, P.-N.; Zheng, J.; Nowick, J. S.; Eisenberg, D. *J. Am. Chem. Soc.* **2011**, *133*, 6736−6744. (b) Liu, C.; Zhao, M.; Jiang, L.; Cheng, P.-N.; Park, J.; Sawaya, M. R.; Pensalfini, A.; Gou, D.; Berk, A. J.; Glabe, C. G.; Nowick, J. S.; Eisenberg, D. *Proc. Natl. Acad. Sci. U.S.A.* **2012**, *109*, 20913−20918.

(26) Stroud, J. C.; Liu, C.; Teng, P. K.; Eisenberg, D. *Proc. Natl. Acad. Sci. U.S.A.* **2012**, *109*, 7717−7722.

(27) (a) Qiang, W.; Yau, W.-M.; Tycko, R. *J. Am. Chem. Soc.* **2011**, *133*, 4018−4029. (b) Qiang, W.; Yau, W.-M.; Luo, Y.; Mattson, M. P.; Tycko, R. *Proc. Natl. Acad. Sci. U.S.A.* **2012**, *109*, 4443−4448.

(28) (a) Tjenberg, L. O.; Tjenberg, A.; Bark, N.; Yuan, S.; Ruzsicska, B. P.; Bu, Z.; Thyberg, J.; Callaway, D. J. E. *Biochem. J.* **2002**, *366*, 343−351. (b) Hoyer, W.; Grönwall, C.; Jonsson, A.; Ståhl, S.; Härd, T. *Proc. Natl. Acad. Sci. U.S.A.* **2008**, *105*, 5099−5104. (c) Sandberg, A.; Luheshi, L. M.; Söllvander, S.; de Barros, T. P.; Macao, B.; Knowles, T. P. J.; Biverstål, H.; Lendel, C.; Ekholm-Petterson, F.; Dubnovitsky, A.; Lannfelt, L.; Dobson, C. M.; Härd, T. *Proc. Natl. Acad. Sci. U.S.A.* **2010**, *107*, 15595−15600.

(29) The fibril-like assemblies of oligomers of macrocyclic β-sheet **3** are largely isolated from each other in crystal lattice, separated by channels containing water. The crystallographic structure may thus provide a model for amyloid oligomers in solution.

(30) (a) Lansbury, P. T., Jr.; Caughey, B. *Chem. Biol.* **1995**, *2*, 1−5. (b) Petkova, A. T.; Leapman, R. D.; Guo, Z.; Yau, W.-M.; Mattson, M. P.; Tycko, R. *Science* **2005**, *307*, 262−265. (c) Cremades, N.; Cohen, S. I.; Deas, E.; Abramov, A. Y.; Chen, A. Y.; Orte, A.; Sandal, M.; Clarke, R. W.; Dunne, P.; Aprile, F. A.; Bertoncini, C. W.; Wood, N. W.; Knowles, T. P.; Dobson, C. M.; Klenerman, D. *Cell* **2012**, *149*, 1048−1059. (d) Soto, C. *Cell* **2012**, *149*, 968−977. (e) Shahnawaz, M.; Soto, C. *J. Biol. Chem.* **2012**, *287*, 11665−11676. (f) Nussbaum, J. M.; Schilling, S.; Cynis, H.; Silva, A.; Swanson, E.; Wangsanut, T.; Tayler, K.; Wiltgen, B.; Hatami, A.; Rönicke, R.; Reymann, K.; Hutter-Paier, B.; Alexandru, A.; Jagla, W.; Graubner, S.; Glabe, C. G.; Demuth, H.-U.; Bloom, G. S. *Nature* **2012**, *485*, 651−655. (g) Morales, R.; Duran-Aniotz, C.; Castilla, J.; Estrada, L. D.; Soto, C. *Mol. Psychiatry* **2012**, *17*, 1347−1353. (h) Watts, J. C.; Condello, C.; Stöhr, J.; Oehler, A.; Lee, J.; DeArmond, S. J.; Lannfelt, L.; Ingelsson, M.; Giles, K.; Prusiner, S. B. *Proc. Natl. Acad. Sci. U.S.A.* **2014**, *111*, 10323−10328. (i) Stöhr, J.; Condello, C.; Watts, J. C.; Bloch, L.; Oehler, A.; Nick, M.; DeArmond, S. J.; Giles, K.; DeGrado, W. F.; Prusiner, S. B. *Proc. Natl. Acad. Sci. U.S.A.* **2014**, *111*, 10329−10334.